Effect of modulated photo-activation on polymerization shrinkage behavior of dental restorative resin composites

Tauböck, Tobias T ; Feilzer, Albert J ; Buchalla, Wolfgang ; Kleverlaan, Cornelis J ; Krejci, Ivo ; Attin, Thomas

Abstract: This study investigated the influence of modulated photo-activation on axial polymerization shrinkage, shrinkage force, and hardening of light- and dual-curing resin-based composites. Three light-curing resin composites (SDR bulk-fill, Esthet X flow, and Esthet X HD) and one dual-curing material (Rebilda DC) were subjected to different irradiation protocols with identical energy density (27 J cm(-2)): high-intensity continuous light (HIC), low-intensity continuous light (LIC), soft-start (SS), and pulse-delay curing (PD). Axial shrinkage and shrinkage force of 1.5-mm-thick specimens were recorded in real time for 15 min using custom-made devices. Knoop hardness was determined at the end of the observation period. Statistical analysis revealed no significant differences among the curing protocols for both Knoop hardness and axial shrinkage, irrespective of the composite material. Pulse-delay curing generated the significantly lowest shrinkage forces within the three light-curing materials SDR bulk-fill, Esthet X flow, and Esthet X HD. High-intensity continuous light created the significantly highest shrinkage forces within Esthet X HD and Rebilda DC, and caused significantly higher forces than LIC within Esthet X flow. In conclusion, both the composite material and the applied curing protocol control shrinkage force formation. Pulse-delay curing decreases shrinkage forces compared with high-intensity continuous irradiation without affecting hardening and axial polymerization shrinkage.

DOI: https://doi.org/10.1111/eos.12139

Effect of modulated photo-activation on polymerization shrinkage behavior of dental restorative resin composites

Tobias T. Tauböck[1], Albert J. Feilzer[2], Wolfgang Buchalla[3], Cornelis J. Kleverlaan[2], Ivo Krejci[4], Thomas Attin[1]

[1]Department of Preventive Dentistry, Periodontology and Cariology, Center for Dental Medicine, University of Zurich, Zurich, Switzerland

[2]Department of Dental Materials Science, Academic Centre for Dentistry Amsterdam (ACTA), University of Amsterdam and VU University Amsterdam, Amsterdam, The Netherlands

[3]Department of Operative Dentistry and Periodontology, University of Regensburg, Regensburg, Germany

[4]Division of Cariology and Endodontology, School of Dentistry, University of Geneva, Geneva, Switzerland

Running title:

Curing protocols: shrinkage behavior and hardening

Corresponding author:

Dr. Tobias T. Tauböck

Department of Preventive Dentistry, Periodontology and Cariology

Center for Dental Medicine, University of Zurich

Plattenstrasse 11, CH-8032 Zurich, Switzerland

Telephone: +41–44–6343448, Telefax: +41–44–6344308

E-mail: tobias.tauboeck@zzm.uzh.ch

Abstract

This study investigated the influence of modulated photo-activation on axial polymerization shrinkage, shrinkage force, and hardening of light- and dual-curing resin-based composites. Three light-curing resin composites (SDR bulk-fill, Esthet X flow, Esthet X HD) and one dual-curing material (Rebilda DC) were subjected to different irradiation protocols with equal energy density (27 J/cm^2): High-intensity continuous light (HIC), low-intensity continuous light (LIC), soft-start (SS) and pulse-delay curing (PD). Axial shrinkage and shrinkage force of 1.5-mm-thick specimens were recorded in real-time for 15 min using custom-made devices. Knoop hardness was determined at the end of the observation period. Statistical analysis revealed no significant differences among the curing protocols for both Knoop hardness and axial shrinkage, irrespective of the composite material. PD generated the significantly lowest shrinkage forces within the three light-curing materials SDR bulk-fill, Esthet X flow and Esthet X HD. HIC created the significantly highest shrinkage forces within Esthet X HD and Rebilda DC, and caused significantly higher forces than LIC within Esthet X flow. In conclusion, both the composite material and the applied curing protocol control shrinkage force formation. Pulse-delay curing decreases shrinkage forces compared to high-intensity continuous irradiation without affecting hardening and axial polymerization shrinkage.

Key words: soft-start, pulse-delay, flowable resin composite, polymerization contraction, shrinkage force

Introduction

During polymerization of dimethacrylate-based composites, the formation of a polymer network is accompanied by an exchange of intermolecular van der Waals links for shorter covalent bonds, causing volumetric shrinkage typically in the range of 1.5 to 5% (1). Clinically, this dimensional change is hindered by the confinement of the material bonded to cavity walls, and, as a result, shrinkage manifests itself as stress. Polymerization shrinkage stress constitutes a major clinical concern because it has the potential to deflect the surrounding tooth structure, which in turn may result in cuspal movement and enamel fracture (2, 3), or initiate microcracking of the restorative material (4). Furthermore, when shrinkage forces exceed bond strength to cavity walls, gaps will develop at the tooth-composite interface, possibly leading to microleakage and ultimately to clinical signs and symptoms ranging from marginal discoloration to post-operative sensitivity and secondary caries (5-8).

The magnitude of contraction stress is dependent not only on the amount of volumetric shrinkage, but also on cavity geometry and compliance of the surrounding bonding substrate, as well as on the material's visco-elastic behavior, characterized by its flow capacity in the early stages of the curing reaction and by the elastic modulus acquired during polymerization (9, 10). Prior to gelation, plastic deformation (or flow) of the resin composite compensates for most of the polymerization shrinkage by the rearrangement of propagating polymer chains. This behavior is responsible for the reduction of stress to levels much lower than the expected theoretical values, which are calculated from elastic modulus and shrinkage strain of the material (11, 12).

Various clinical approaches have been proposed in an attempt to minimize shrinkage stress, including incremental layering techniques (13), the use of low-modulus liners as stress absorbing intermediate layers (14, 15), and the application of modulated photo-activation methods involving low initial irradiance as a way to reduce the rate of polymerization (16, 17). In theory, a polymer network developing at a slower rate would stay

longer in the pre-gel stage, and consequently more time would be available for viscous flow to occur, postponing the onset of stress development and reducing its magnitude (18). Indeed, soft-start curing, where a low irradiance is applied during the first part of the polymerization period before switching to higher irradiance for the remaining curing time, and pulse-delay curing, being similar to the soft-start routine except that a waiting period ('relaxation interval') is introduced between the initial low-irradiance and the following high-irradiance polymerization, have been shown to decrease contraction stress and improve restoration interfacial integrity when compared to continuous high-intensity photo-activation, without compromising the material's physical properties (16, 19-21). On the other hand, stress decrease provided by irradiation at reduced initial intensity has also been associated with a concurrent reduction in the degree of carbon double-bond conversion (22), which in turn might deteriorate the mechanical properties and biocompatibility of the resin composite restoration (23, 24).

Curing characteristics vary depending on material composition (25), which may influence the efficacy of photo-activation protocols with modulated irradiation. A study evaluating the influence of low initial irradiance curing approaches on shrinkage stress development of three commercial light-curing materials found stress reductions between 19 and 30% when compared with continuous high-intensity light exposure using similar energy density (26). The effectiveness of soft-start and pulse-delay curing on polymerization shrinkage and contraction stress of dual-curing resin composites still needs to be determined.

Besides managing light exposure, the dynamics of the polymerization reaction may also be controlled by modifications in the resin composite formulation. Recently, the incorporation of a polymerization modulator in a high molecular weight urethane-based methacrylate resin has been shown to delay gelation (27), thereby increasing the opportunity for stress relief by flow. Investigations on the shrinkage behavior of resin systems based on this so-called SDR ("Stress Decreasing Resin") technology revealed that these materials generated significantly lower contraction forces than conventional flowable and hybrid resin

composites when being photo-activated using continuous high-intensity irradiation (27, 28). To date, no information is available in the literature on the effects of low irradiance curing regimens on the shrinkage kinetics of resin composites with SDR technology.

Based on these considerations, the aim of the present study was to investigate the influence of modulated photo-activation methods (continuous low-intensity, soft-start, pulse-delay) on axial polymerization shrinkage and shrinkage force of various dimethacrylate-based resin composite materials: three light-curing resin composites (including a flowable composite based on the SDR technology, a conventional flowable composite, as well as a regular microhybrid composite) and one dual-curing composite material. In addition, microhardness (as an indirect measure of the degree of conversion) was determined in order to allow an assessment of the physical properties of the set materials. It was hypothesized that modulated photo-activation would result in reduced shrinkage force formation compared to high-intensity continuous irradiation, without affecting axial shrinkage and hardening of the resin composite materials.

Materials and methods

Four commercial resin composite materials were used in this study: a light-curing microhybrid flowable composite having incorporated a polymerization modulator within the resin matrix (SDR; Dentsply DeTrey, Konstanz, Germany), a conventional light-curing microhybrid flowable composite (Esthet X flow; Dentsply DeTrey), the high viscosity counterpart of the conventional flowable composite (Esthet X HD; Dentsply DeTrey), and a dual-curing microhybrid flowable composite (Rebilda DC; VOCO, Cuxhaven, Germany). Details of the test materials are presented in Table 1. In all experiments, the composite specimens were photo-activated with a LED light-curing unit (Bluephase; Ivoclar Vivadent, Schaan, Liechtenstein) used in the High-Intensity Mode and equipped with a focusing (Power-Booster) light guide with an 8-mm diameter light emission window. The emission spectrum (Fig. 1) of the curing unit was measured by means of a fiber optic spectrometer (HR2000; Ocean Optics, Dunedin, FL, USA) containing a high-resolution CCD array detector (ILX511; Sony, Tokyo, Japan). Four light-curing protocols (Table 2), each employing a standardized energy density of 27 J/cm^2, were investigated in the following tests. The different irradiances were obtained by changing the distance of the light guide tip to the specimen surface. The desired irradiances at the top surface of the composite specimens were verified using a PM2 thermopile sensor and calibrated FieldMaxII-TO power meter (Coherent, Santa Clara, CA, USA).

Axial shrinkage

Axial shrinkage was measured with a custom-made device (Fig. 2), described in detail previously (29, 30). In brief, it consisted of a sturdy metal frame, upon which a thin aluminum platelet with a perpendicular diaphragm was loosely placed. The edge of the diaphragm extended into a recess in an infrared measuring sensor. A standardized volume (42 mm^3) of the resin composite material to be investigated was placed on the aluminum platelet with the aid of a cylindrical Teflon mold. The material was then carefully flattened to a test height of 1.5 mm by means of a sandblasted (50 µm Al_2O_3) and silanized (Monobond Plus;

Ivoclar Vivadent) glass plate. Photo-activation of the composite materials was performed through the glass plate according to the protocols described in Table 2. The reduction in light intensity when the curing light passes through the glass plate was measured and amounted to 10%. This loss was compensated in all curing protocols in order to ensure that the desired irradiances were reached at the top surface of the composite specimens. The vertical movement of the diaphragm caused by polymerization shrinkage of the test materials was detected by the temperature-compensated infrared sensor with an accuracy of 0.1 µm at a sampling frequency of 5 Hz. Measurements were carried out for 15 min from the initiation of photo-activation at an ambient room temperature of 25 ± 1°C. Data were transferred real-time to a personal computer (Macintosh IIfx; Apple Computer, Cupertino, CA, USA) by means of an A/D converter using custom-made software. Six replicate measurements were conducted for each experimental condition.

Shrinkage force

Measurements of polymerization shrinkage force were carried out using a custom-made device (Fig. 3) that was also described in detail previously (29, 30). In brief, the upper part of the apparatus consisted of a semi-rigid load cell (PM 11-K; Mettler, Greifensee, Switzerland; instrument compliance: 0.4 µm/N), to which a metal cylinder was screwed. The cylinder was coated with a standardized volume (42 mm^3) of test material, which was compressed to a thickness of 1.5 mm, and a surface area of 28 mm^2 at the top and at the bottom of the specimen (corresponding to a ratio of bonded to unbonded surface area, i.e. C-factor, of 2.0), by means of a glass plate attached to the base of the device. To improve adhesion, the surfaces of the metal cylinder and of the glass plate were sandblasted with 50 µm Al_2O_3 and primed or silanized (Monobond Plus; Ivoclar Vivadent). Light-curing was performed according to Table 2 through the glass plate, via a recess in the lower frame, again considering a reduction of 10% in light intensity when the curing light passes through the glass plate. The forces generated during polymerization shrinkage were detected by means of the load cell at a sampling frequency of 5 Hz. Measurements were carried out for 15 min

from the initiation of photo-activation at an ambient room temperature of 25 ± 1°C. Data were transferred real-time to the attached computer (Macintosh IIfx; Apple Computer) via an A/D converter using custom-made software. Six replicate measurements were conducted for each experimental condition.

Microhardness

Determination of microhardness as an indirect measure of degree of conversion was performed as previously described in the literature (29, 31). The same volume (42 mm^3) of test material as for evaluation of axial shrinkage and shrinkage force was placed on a glass plate and compressed between spacers of 1.6 mm by means of a second, sandblasted (50 µm Al_2O_3) and silanized (Monobond Plus; Ivoclar Vivadent) glass plate. Light-curing was performed according to Table 2 through the pretreated glass plate covering the top surface of the specimen, again considering a reduction of 10% in light intensity when the curing light passes through the glass plate. Six specimens were prepared for each experimental condition and stored dry at an ambient room temperature of 25 ± 1°C in the dark until testing. Prior to testing, a layer of 0.1 mm, as verified with a digital caliper (CAPA 150; Tesa SA, Renens, Switzerland), was removed from the non-irradiated composite surface (bottom surface) by wet grinding with silicon carbide (SiC) paper up to grain-size 4000 (FEPA P standard). Knoop hardness (KHN) was measured 15 min after the start of photo-activation using a digital microhardness tester (model no. 1600-6106; Buehler, Lake Bluff, IL, USA). For each specimen, three indentations were performed under a load of 10 g applied for 20 s at random positions around the center of the non-irradiated surface, and the average of the three readings was calculated.

Statistical analysis

After confirming the validity of the assumption of normality by means of the Kolmogorov-Smirnov and Shapiro-Wilk tests, data at the end of the 15-min observation period were analyzed using analysis of variance (ANOVA) followed by Scheffé's post-hoc test to identify

pairwise differences. All tests were conducted at a pre-set global significance level of $\alpha = 0.05$ (SPSS Version 20; SPSS, Chicago, IL, USA).

Results

Fig. 4 shows the development of axial polymerization shrinkage for each experimental condition as a function of time. The axial shrinkage values obtained at the end of the 15-min observation period are presented in Table 3. Two-way ANOVA revealed significant differences in axial shrinkage among composite materials ($P < 0.001$) but not among photo-activation protocols ($P = 0.153$), and no interaction effects between photo-activation protocols and composite materials ($P = 0.117$). Esthet X HD caused the significantly lowest axial polymerization shrinkage, followed by SDR, Rebilda DC and Esthet X flow with all curing protocols.

Fig. 5 shows the time-dependant development of shrinkage force during 15 min for each experimental condition. The initial course of shrinkage force formation is detailed in Fig. 6. The shrinkage force values obtained at the end of the 15-min observation period are presented in Table 4. Two-way ANOVA revealed significant differences in shrinkage force due to both composite material ($P < 0.001$) and photo-activation protocol ($P < 0.001$), and significant differences were also found for the interaction between these two factors ($P < 0.001$). PD generated the significantly lowest shrinkage forces within the three light-curing resin composites SDR, Esthet X flow and Esthet X HD, but did not result in significantly lower shrinkage force formation compared to LIC and SS within dual-curing Rebilda DC. HIC created the significantly highest shrinkage forces within Esthet X HD and Rebilda DC, and LIC produced lower shrinkage forces than HIC within Esthet X flow. SDR generated the significantly lowest shrinkage forces when HIC was used, while Esthet X HD caused the significantly lowest shrinkage forces for PD.

Knoop hardness for the different combinations of composite materials and curing protocols, observed 15 min after the start of photo-activation, are displayed in Fig. 7. For each material tested, no significant differences in the degree of hardness were observed among the curing protocols.

Discussion

Free-radical photo-polymerization of resin composites causes a gelation in which the material is transformed from a viscous-plastic to a more densely packed rigid-elastic structure with reduced intermolecular distances (10). The resulting volumetric shrinkage has been reported to continue for up to about 24 h after photo-activation (32). Nevertheless, real-time shrinkage and shrinkage stress measurements are usually limited to the first 3–30 min of the polymerization reaction, in order to shorten overall measurement duration (17, 19, 33-37). In the present study, the development of axial polymerization shrinkage and shrinkage force were continuously followed for 15 min, based on preliminary investigations in our laboratory, which revealed that after 15 min both properties had reached over 86% of their maximum values after 24 h, irrespective of the tested composite material. Furthermore, relative differences in post-gel shrinkage strains of resin composites exposed to different curing scenarios have been shown to remain constant after the first 5 min post-irradiation (38). Therefore, although current data do not reflect the ultimate values of axial shrinkage and shrinkage force in absolute terms, their use as a means to compare different photo-activation protocols, as well as to estimate final values of the measured properties, is justified.

For a given material and test configuration, absolute values of contraction stress are influenced by the compliance of the measurement system (39). Near-zero compliance testing set-ups, containing feedback systems in order to maintain the original specimen height throughout the experiment, might overestimate stress values, because deformation of dental substrates would relieve part of the shrinkage forces (9, 40). In the experimental design of the current investigation, axial specimen deformation was only partially restricted because the load cell was axially displaced by 0.4 μm/N, resulting in a maximum deformation of 17 μm. In this way, a semi-rigid configuration of a cavity with a C-factor of 2.0 was simulated. Several studies have revealed that the cusps of premolars and molars deflect inwards after the placement of Class II resin composite restorations, with the amount of intercuspal narrowing ranging from 11 to 46 μm (41-43), thus justifying the experimental set-up in the

present research.

In the shrinkage stress test only the forces developing uniaxially, in the long axis of the specimen, are registered, even though the shrinking composite develops a triaxial stress state (9, 44). Within a cavity, the loading condition is multiaxial, because, in contrast to the configuration in the testing device, the composite material is not simply bonded to two opposing surfaces, but to the cavity floor and walls, resulting in a very heterogeneous stress distribution in the resin composite restoration (44, 45). Furthermore, in cavities with a high ratio of bonded to unbonded surface area, e.g. Class I cavities, stress relief by viscous flow is hindered (12), which might result in higher shrinkage stresses compared to those measured in the current test set-up. In contrast, shrinkage stresses generated by resin composite restorations bonded to a flat tooth surface (minimal constrained surface area), i.e. Class IV restorations, might be lower than those recorded in the present study.

The first part of the hypothesis that modulated photo-activation would result in reduced shrinkage force formation compared to high-intensity continuous irradiation was accepted for pulse-delay curing, but was only partially accepted for soft-start curing and low-intensity continuous irradiation because these protocols reduced shrinkage forces only for some but not for all of the composite materials tested. Shrinkage stress development in resin composites is related to reaction kinetics with the rate of polymerization being proportional to the square root of the irradiance absorbed by the material (46, 47). When irradiation is started at lower irradiance values, a reduced number of polymer growth centers is activated at the same time, reducing the reaction rate and decreasing stress generation due to the increased opportunity for viscous flow and chain relaxation before mobility is restricted by vitrification (18). Shrinkage force curves (Fig. 6) indicate that the tested modulated curing protocols succeeded in postponing the onset of stress build-up, lending support to the hypothesis of increased pre-gel flow capacity (and consequently non-rigid shrinkage) when reducing irradiance during photo-polymerization. Nevertheless, soft-start curing and low-intensity continuous irradiation reduced final shrinkage forces not for all of the composite materials tested (Table 4, Fig. 5). The different response of resin composites to modulated

photo-activation might be due to compositional differences. Photo-initiator and inhibitor concentrations, monomer blending and filler content have been shown to affect resin reactivity (25, 48, 49), which might have affected stress relief effectiveness of the modulated curing protocols.

The present results show that pulse-delay curing was effective in reducing shrinkage force formation when compared to continuous high-intensity irradiation, irrespective of the composite material. Furthermore, within the three light-curing resin composites tested, the pulse-delay technique generated lower polymerization forces than both soft-start and low-intensity continuous curing (Table 4, Fig. 5). The low energy density imparted to the composites during the initial light-activation pulse (0.9 J/cm^2) might have produced low initial monomer conversion and maintained a high level of molecular mobility within the polymer matrix (1). During the light-off period before the second light exposure, the polymerization process is slow, because no new radicals are generated in light-curing resin composites from initiation, and the reaction progresses as a result of the 'dark-cure' reaction being characterized by chain propagation of already existing structures (11). The slow polymerization rate during this period might have prolonged the early low modulus phase, thus allowing more time for molecular rearrangement and stress relief. In contrast to the light-curing materials, the dual-curing resin composite did not benefit from the pulse-delay curing regimen regarding shrinkage force relief when compared with the other modulated irradiation protocols (soft-start curing, low-intensity continuous curing) under investigation. This might be due to the additional autopolymerizing mechanism of dual-curing Rebilda DC, which is based on a redox reaction of benzoyl peroxide with a tertiary aromatic amine (N,N-Bis-hydroxyethyl-p-toluidine). This reaction generates free radicals and thus initiates polymerization in the absence of light, which might have added to elastic modulus development during the light-off period and decreased flow capacity. Indeed, shrinkage force curves (Fig. 5) indicate greater force development during the light-off period of the pulse-delay protocol for the dual-curing material compared to the light-curing resin composites.

The flowable bulk-fill material SDR generated significantly lower shrinkage forces

compared to the conventional flowable and microhybrid resin composites examined when irradiation was performed at continuous high irradiance (Table 4), even though axial polymerization shrinkage of the SDR composite exceeded that of microhybrid Esthet X HD (Table 3, Fig. 4). A recent study observed reduced shrinkage stress formation for SDR not only when compared to regular methacrylate-based resin composites, but also compared to a low-shrinkage silorane-based composite material (Filtek Silorane) (27). The composition of SDR features a so-called 'polymerization modulator', a chemical moiety which is embedded in the center of the polymerizable urethane dimethacrylate resin backbone of the material. Due to the conformational flexibility around the centered modulator, the monomers are supposed to link more flexibly to form the polymer network, thereby allowing for internal stress relaxation without harming degree of conversion (28). Interestingly, the present results revealed no benefit of SDR over the conventional microhybrid composite material Esthet X HD regarding shrinkage force generation when modulated curing protocols with low initial irradiance were applied (Table 4), and therefore do not confirm the results obtained with high-intensity continuous irradiation. This might be explained by the relatively low responsiveness of SDR to modulated photo-activation, probably due to the predominant effect of the polymerization modulator on reaction kinetics and stress development of the material.

The equal chemical composition of the resin matrix of high-viscosity Esthet X HD and low-viscosity Esthet X flow (Table 1) offers the possibility to directly elucidate the effect of filler content on shrinkage patterns. Our results indicate that the higher filled resin composite (Esthet X HD; filler content: 60 vol%) caused significantly less polymerization shrinkage than its flowable counterpart (Esthet X flow; filler content: 53 vol%) (Table 3, Fig. 4). A strong inverse correlation between filler percent and shrinkage strain has been previously established, which might be explained by the fact that at higher filler levels, the volume occupied by organic matrix and, therefore, the number of reactive methacrylate groups decreases (50). On the other hand, the stiffness of the composite material is also increased at higher filler levels (51), which leads to increased stress at a given shrinkage strain,

according to Hooke's law. Nevertheless, in the present study, the higher filled material generated significantly lower shrinkage forces (Table 4) due to its reduced polymerization contraction. Indeed, a direct relationship between volumetric shrinkage and polymerization stress, and an inverse relationship between filler content and polymerization stress has been established in semi-rigid testing systems (52).

Axial polymerization shrinkage of the flowable resin composites under investigation was higher compared to non-flowable Esthet X HD, and increased in the following order: SDR < Rebilda DC < Esthet X flow (Table 3, Fig. 4). The low polymerization shrinkage of SDR might result from the large size of its base monomer, which is a modified UDMA and has a high molecular weight in comparison with Bis-GMA and traditional UDMA (849 g/mole vs. 512 g/mole vs. 471 g/mole, respectively) enabling the resin to exhibit a lower density of reactive sites per unit mass of material (53, 54). The lower shrinkage of Rebilda DC compared to Esthet X flow might be explained by the higher filler content of Rebilda DC and its TEGDMA-free resin composition. TEGDMA is a highly reactive diluent monomer with flexible aliphatic units, which due to its favorable stereochemistry exhibits higher values of degree of conversion compared with Bis-GMA, EBPADMA and UDMA, thus leading to greater shrinkage (55-57). Furthermore, unlike Esthet X flow, Rebilda DC contains DDDMA in its resin matrix. This monomer has been shown to cause low shrinkage during polymerization due to a long organic spacer between two reactive end methacrylate groups (58).

The second part of the hypothesis that modulated photo-activation would not affect axial polymerization shrinkage and hardening of the composite materials was confirmed by the results. Volumetric shrinkage of resin composites has been shown to be proportional to the degree of conversion (46), which, in turn, is related to the total light energy density, i.e., the product of irradiance and exposure time delivered to the composite during photo-activation (59). In the current study, Knoop hardness was used as an indirect measure of the degree of conversion of a specific resin composite (60, 61), based on its proven correlation with infrared spectroscopy (62-66). The similar microhardness and axial

shrinkage observed when the materials were irradiated according to the different curing protocols might be due to the fact that the same energy density (27 J/cm^2) was delivered by all photo-activation methods, and provides further evidence for a reciprocal relationship between irradiance and exposure time on conversion of resin-based composites (67). Therefore, since differences in contraction forces cannot be accounted for by differences in extent of cure or polymerization shrinkage, it may be assumed that the composite's increased flow capacity was the governing factor for the reduced shrinkage force formation attained with modulated photo-activation. In contrast to our findings, LU *et al.* (22) observed that a decrease in contraction stress provided by low initial irradiance curing protocols is accompanied by reduced final monomer conversion, even if the applied energy density is similar to that of a standard, full-irradiance protocol. Stress reduction achieved at the expense of the degree of conversion is clinically undesirable, because low monomer conversion might not only compromise the material's mechanical properties (24), but also reduce biocompatibility (23). In the above-mentioned study, noting a decrease in final conversion after modulated photo-activation (22), irradiation was started at a rather low irradiance of 100 mW/cm^2, representing thus only one third of the irradiance used for initial irradiation in the current investigation. It might be that for very low irradiances exposure reciprocity does not hold (18), which could explain the contradicting findings of the studies.

Based on the results of the present *in vitro* study, it can be concluded that both the composite material and the applied light-curing protocol control shrinkage force formation. Pulse-delay curing reduces shrinkage forces compared to irradiation at continuous high irradiance, without affecting axial polymerization shrinkage and without compromising the degree of hardening of the investigated light- and dual-curing resin composites. The tested regular (high viscosity) composite material seems to profit most from the pulse-delay technique regarding shrinkage force relief.

Acknowledgements – The authors thank Dr. Malgorzata Roos, Biostatistics Unit, Institute of Social and Preventive Dentistry, University of Zurich, for her statistical advice, and Dentsply DeTrey for providing the composite materials.

Conflicts of interests – The authors declare that they have no conflicts of interest.

References

1. FERRACANE JL. Developing a more complete understanding of stresses produced in dental composites during polymerization. *Dent Mater* 2005; **21:** 36-42.
2. TANTBIROJN D, VERSLUIS A, PINTADO MR, DELONG R, DOUGLAS WH. Tooth deformation patterns in molars after composite restoration. *Dent Mater* 2004; **20:** 535-542.
3. JÖRGENSEN KD, ASMUSSEN E, SHIMOKOBE H. Enamel damages caused by contracting restorative resins. *Scand J Dent Res* 1975; **83:** 120-122.
4. EICK JD, WELCH FH. Polymerization shrinkage of posterior composite resins and its possible influence on postoperative sensitivity. *Quintessence Int* 1986; **17:** 103-111.
5. TOTIAM P, GONZALEZ-CABEZAS C, FONTANA MR, ZERO DT. A new in vitro model to study the relationship of gap size and secondary caries. *Caries Res* 2007; **41:** 467-473.
6. CALHEIROS FC, SADEK FT, BRAGA RR, CARDOSO PE. Polymerization contraction stress of low-shrinkage composites and its correlation with microleakage in class V restorations. *J Dent* 2004; **32:** 407-412.
7. PEUTZFELDT A, ASMUSSEN E. Determinants of in vitro gap formation of resin composites. *J Dent* 2004; **32:** 109-115.
8. CARVALHO RM, PEREIRA JC, YOSHIYAMA M, PASHLEY DH. A review of polymerization contraction: the influence of stress development versus stress relief. *Oper Dent* 1996; **21:** 17-24.
9. BRAGA RR, BALLESTER RY, FERRACANE JL. Factors involved in the development of polymerization shrinkage stress in resin-composites: a systematic review. *Dent Mater* 2005; **21:** 962-970.
10. DAVIDSON CL, FEILZER AJ. Polymerization shrinkage and polymerization shrinkage stress in polymer-based restoratives. *J Dent* 1997; **25:** 435-440.
11. LU H, STANSBURY JW, BOWMAN CN. Towards the elucidation of shrinkage stress development and relaxation in dental composites. *Dent Mater* 2004; **20:** 979-986.
12. FEILZER AJ, DE GEE AJ, DAVIDSON CL. Quantitative determination of stress reduction by flow in composite restorations. *Dent Mater* 1990; **6:** 167-171.

13. PARK J, CHANG J, FERRACANE J, LEE IB. How should composite be layered to reduce shrinkage stress: incremental or bulk filling? *Dent Mater* 2008; **24:** 1501-1505.
14. KORKMAZ Y, OZEL E, ATTAR N. Effect of flowable composite lining on microleakage and internal voids in Class II composite restorations. *J Adhes Dent* 2007; **9:** 189-194.
15. CHOI KK, CONDON JR, FERRACANE JL. The effects of adhesive thickness on polymerization contraction stress of composite. *J Dent Res* 2000; **79:** 812-817.
16. ILIE N, JELEN E, HICKEL R. Is the soft-start polymerisation concept still relevant for modern curing units? *Clin Oral Investig* 2011; **15:** 21-29.
17. KREJCI I, PLANINIC M, STAVRIDAKIS M, BOUILLAGUET S. Resin composite shrinkage and marginal adaptation with different pulse-delay light curing protocols. *Eur J Oral Sci* 2005; **113:** 531-536.
18. SAKAGUCHI RL, WILTBANK BD, MURCHISON CF. Contraction force rate of polymer composites is linearly correlated with irradiance. *Dent Mater* 2004; **20:** 402-407.
19. CUNHA LG, ALONSO RC, PFEIFER CS, CORRER-SOBRINHO L, FERRACANE JL, SINHORETI MA. Contraction stress and physical properties development of a resin-based composite irradiated using modulated curing methods at two C-factor levels. *Dent Mater* 2008; **24:** 392-398.
20. KANCA J 3RD, SUH BI. Pulse activation: reducing resin-based composite contraction stresses at the enamel cavosurface margins. *Am J Dent* 1999; **12:** 107-112.
21. MEHL A, HICKEL R, KUNZELMANN KH. Physical properties and gap formation of light-cured composites with and without 'softstart-polymerization'. *J Dent* 1997; **25:** 321-330.
22. LU H, STANSBURY JW, BOWMAN CN. Impact of curing protocol on conversion and shrinkage stress. *J Dent Res* 2005; **84:** 822-826.
23. CAUGHMAN WF, CAUGHMAN GB, SHIFLETT RA, RUEGGEBERG F, SCHUSTER GS. Correlation of cytotoxicity, filler loading and curing time of dental composites. *Biomaterials* 1991; **12:** 737-740.

24. FERRACANE JL, GREENER EH. The effect of resin formulation on the degree of conversion and mechanical properties of dental restorative resins. *J Biomed Mater Res* 1986; **20:** 121-131.

25. FEILZER AJ, DAUVILLIER BS. Effect of TEGDMA/BisGMA ratio on stress development and viscoelastic properties of experimental two-paste composites. *J Dent Res* 2003; **82:** 824-828.

26. LIM BS, FERRACANE JL, SAKAGUCHI RL, CONDON JR. Reduction of polymerization contraction stress for dental composites by two-step light-activation. *Dent Mater* 2002; **18:** 436-444.

27. ILIE N, HICKEL R. Investigations on a methacrylate-based flowable composite based on the SDR technology. *Dent Mater* 2011; **27:** 348-355.

28. RULLMANN I, SCHATTENBERG A, MARX M, WILLERSHAUSEN B, ERNST CP. Photoelastic determination of polymerization shrinkage stress in low-shrinkage resin composites. *Schweiz Monatsschr Zahnmed* 2012; **122:** 294-299.

29. TAUBÖCK TT, BORTOLOTTO T, BUCHALLA W, ATTIN T, KREJCI I. Influence of light-curing protocols on polymerization shrinkage and shrinkage force of a dual-cured core build-up resin composite. *Eur J Oral Sci* 2010; **118:** 423-429.

30. STAVRIDAKIS MM, LUTZ F, JOHNSTON WM, KREJCI I. Linear displacement and force induced by polymerization shrinkage of resin-based restorative materials. *Am J Dent* 2003; **16:** 431-438.

31. HOFMANN N, HUGO B, KLAIBER B. Effect of irradiation type (LED or QTH) on photo-activated composite shrinkage strain kinetics, temperature rise, and hardness. *Eur J Oral Sci* 2002; **110:** 471-479.

32. TRUFFIER-BOUTRY D, DEMOUSTIER-CHAMPAGNE S, DEVAUX J, BIEBUYCK JJ, MESTDAGH M, LARBANOIS P, LELOUP G. A physico-chemical explanation of the post-polymerization shrinkage in dental resins. *Dent Mater* 2006; **22:** 405-412.

33. GONCALVES F, PFEIFER CC, STANSBURY JW, NEWMAN SM, BRAGA RR. Influence of matrix composition on polymerization stress development of experimental composites. *Dent Mater* 2010; **26:** 697-703.

34. CADENARO M, MARCHESI G, ANTONIOLLI F, DAVIDSON C, DE STEFANO DORIGO E, BRESCHI L. Flowability of composites is no guarantee for contraction stress reduction. *Dent Mater* 2009; **25:** 649-654.

35. VISVANATHAN A, ILIE N, HICKEL R, KUNZELMANN KH. The influence of curing times and light curing methods on the polymerization shrinkage stress of a shrinkage-optimized composite with hybrid-type prepolymer fillers. *Dent Mater* 2007; **23:** 777-784.

36. KLEVERLAAN CJ, FEILZER AJ. Polymerization shrinkage and contraction stress of dental resin composites. *Dent Mater* 2005; **21:** 1150-1157.

37. SILIKAS N, ELIADES G, WATTS DC. Light intensity effects on resin-composite degree of conversion and shrinkage strain. *Dent Mater* 2000; **16:** 292-296.

38. ERNST CP, BRAND N, FROMMATOR U, RIPPIN G, WILLERSHAUSEN B. Reduction of polymerization shrinkage stress and marginal microleakage using soft-start polymerization. *J Esthet Restor Dent* 2003; **15:** 93-103; discussion 104.

39. LEE SH, CHANG J, FERRACANE J, LEE IB. Influence of instrument compliance and specimen thickness on the polymerization shrinkage stress measurement of light-cured composites. *Dent Mater* 2007; **23:** 1093-1100.

40. WATTS DC, MAROUF AS, AL-HINDI AM. Photo-polymerization shrinkage-stress kinetics in resin-composites: methods development. *Dent Mater* 2003; **19:** 1-11.

41. SULIMAN AA, BOYER DB, LAKES RS. Interferometric measurements of cusp deformation of teeth restored with composites. *J Dent Res* 1993; **72:** 1532-1536.

42. LUTZ F, KREJCI I, BARBAKOW F. Quality and durability of marginal adaptation in bonded composite restorations. *Dent Mater* 1991; **7:** 107-113.

43. PEARSON GJ, HEGARTY SM. Cusp movement in molar teeth using dentine adhesives and composite filling materials. *Biomaterials* 1987; **8:** 473-476.

44. LAUGHLIN GA, WILLIAMS JL, EICK JD. The influence of system compliance and sample geometry on composite polymerization shrinkage stress. *J Biomed Mater Res* 2002; **63:** 671-678.

45. KINOMOTO Y, TORII M. Photoelastic analysis of polymerization contraction stresses in resin composite restorations. *J Dent* 1998; **26:** 165-171.

46. BRAGA RR, FERRACANE JL. Contraction stress related to degree of conversion and reaction kinetics. *J Dent Res* 2002; **81:** 114-118.

47. ODIAN G. *Principles of polymerization.* 3rd ed. New York: John Wiley & Sons, 1991.

48. GONCALVES F, AZEVEDO CL, FERRACANE JL, BRAGA RR. BisGMA/TEGDMA ratio and filler content effects on shrinkage stress. *Dent Mater* 2011; **27:** 520-526.

49. VENHOVEN BA, DE GEE AJ, DAVIDSON CL. Light initiation of dental resins: dynamics of the polymerization. *Biomaterials* 1996; **17:** 2313-2318.

50. BAROUDI K, SALEH AM, SILIKAS N, WATTS DC. Shrinkage behaviour of flowable resin-composites related to conversion and filler-fraction. *J Dent* 2007; **35:** 651-655.

51. BRAEM M, FINGER W, VAN DOREN VE, LAMBRECHTS P, VANHERLE G. Mechanical properties and filler fraction of dental composites. *Dent Mater* 1989; **5:** 346-348.

52. GONCALVES F, KAWANO Y, BRAGA RR. Contraction stress related to composite inorganic content. *Dent Mater* 2010; **26:** 704-709.

53. NAOUM SJ, ELLAKWA A, MORGAN L, WHITE K, MARTIN FE, LEE IB. Polymerization profile analysis of resin composite dental restorative materials in real time. *J Dent* 2012; **40:** 64-70.

54. FERRACANE JL. Resin composite–State of the art. *Dent Mater* 2011; **27:** 29-38.

55. GONCALVES F, PFEIFER CS, FERRACANE JL, BRAGA RR. Contraction stress determinants in dimethacrylate composites. *J Dent Res* 2008; **87:** 367-371.

56. PFEIFER CS, FERRACANE JL, SAKAGUCHI RL, BRAGA RR. Factors affecting photopolymerization stress in dental composites. *J Dent Res* 2008; **87:** 1043-1047.

57. SIDERIDOU I, TSERKI V, PAPANASTASIOU G. Effect of chemical structure on degree of conversion in light-cured dimethacrylate-based dental resins. *Biomaterials* 2002; **23:** 1819-1829.

58. SWIDERSKA J, CZECH Z, KOWALCZYK A. Polymerization shrinkage by investigation of uv curable dental restorative composites containing multifunctional methacrylates. *Pol J Chem Tech* 2013; **15:** 81-85.

59. CALHEIROS FC, DARONCH M, RUEGGEBERG FA, BRAGA RR. Influence of irradiant energy on degree of conversion, polymerization rate and shrinkage stress in an experimental resin composite system. *Dent Mater* 2008; **24:** 1164-1168.

60. TAUBÖCK TT, OBERLIN H, BUCHALLA W, ROOS M, ATTIN T. Comparing the effectiveness of self-curing and light curing in polymerization of dual-cured core buildup materials. *J Am Dent Assoc* 2011; **142:** 950-956.

61. TAUBÖCK TT, BUCHALLA W, HILTEBRAND U, ROOS M, KREJCI I, ATTIN T. Influence of the interaction of light- and self-polymerization on subsurface hardening of a dual-cured core build-up resin composite. *Acta Odontol Scand* 2010; **69:** 41-47.

62. TORRES S, SILVA G, MARIA D, CAMPOS W, MAGALHAES C, MOREIRA A. Degree of conversion and hardness of a silorane-based composite resin: effect of light-curing unit and depth. *Oper Dent* 2014; **39:** E137-E146.

63. PRICE RB, WHALEN JM, PRICE TB, FELIX CM, FAHEY J. The effect of specimen temperature on the polymerization of a resin-composite. *Dent Mater* 2011; **27:** 983-989.

64. RUEGGEBERG FA, CRAIG RG. Correlation of parameters used to estimate monomer conversion in a light-cured composite. *J Dent Res* 1988; **67:** 932-937.

65. DEWALD JP, FERRACANE JL. A comparison of four modes of evaluating depth of cure of light-activated composites. *J Dent Res* 1987; **66:** 727-730.

66. FERRACANE JL. Correlation between hardness and degree of conversion during the setting reaction of unfilled dental restorative resins. *Dent Mater* 1985; **1:** 11-14.

67. HALVORSON RH, ERICKSON RL, DAVIDSON CL. Energy dependent polymerization of resin-based composite. *Dent Mater* 2002; **18:** 463-469.

Figure legends

Fig. 1. Light spectrum profile emitted by the LED curing unit (Bluephase; Ivoclar Vivadent) used in the study.

Fig. 2. Diagram of the measuring device for axial shrinkage. A: Metal frame; B: Aluminum platelet; C: Diaphragm; D: Infrared measuring sensor; E: Composite specimen; F: Glass plate; G: Aluminum plate; H: Curing light tip.

Fig. 3. Diagram of the measuring device for shrinkage force. A: Upper part of measuring device; B: Lower part of measuring device; C: Load cell; D: Metal cylinder; E: Composite specimen; F: Glass plate; G: Holder of glass plate; H: Curing light tip.

Fig. 4. Mean axial shrinkage curves of the composite materials for each photo-activation method as a function of time (n = 6).

Fig. 5. Mean shrinkage force curves of the composite materials for each photo-activation method as a function of time (n = 6). (A) SDR; (B) Esthet X flow; (C) Esthet X HD; (D) Rebilda DC.

Fig. 6. Mean shrinkage force curves of the composite materials for each photo-activation method within 30 s after the start of irradiation (expanded area of Fig. 5). (A) SDR; (B) Esthet X flow; (C) Esthet X HD; (D) Rebilda DC.

Fig. 7. Mean Knoop hardness values and standard deviations (represented by error bars) of all experimental groups at 15 min after the start of irradiation (n = 6). Within each composite material, groups linked with a horizontal bar are not significantly different at the 0.05 level (Scheffé's post-hoc test).

Table 1 – *Manufacturers' information about the resin composite materials used in the study*

Material	Composition	Filler size (μm)	Filler content (wt%/vol%)	Lot no.	Manufacturer
SDR	Resin: Modified UDMA, EBPADMA, TEGDMA Filler: Ba-Al-F-B-Si-glass, Sr-Al-F-Si-glass	0.02–10 (mean 4.2)	68/45	110619	Dentsply DeTrey, Konstanz, Germany
Esthet X flow	Resin: Bis-GMA adduct, EBPADMA, TEGDMA Filler: Ba-F-Al-B-Si-glass, silica	0.02–7.5 (mean 1.2)	61/53	110617	Dentsply DeTrey, Konstanz, Germany
Esthet X HD	Resin: Bis-GMA adduct, EBPADMA, TEGDMA Filler: Ba-F-Al-B-Si-glass, silica	0.02–3 (mean 0.61)	76/60	1105311	Dentsply DeTrey, Konstanz, Germany
Rebilda DC	Resin: Bis-GMA, UDMA, DDDMA Filler: Ba-F-B-Si-glass, silica	0.05–20 (mean 1.5)	71/57	1202575	VOCO, Cuxhaven, Germany

Bis-GMA: Bisphenol-A-glycidyldimethacrylate; DDDMA: Dodecanediol dimethacrylate; EBPADMA: Ethoxylated bisphenol-A-dimethacrylate; TEGDMA: Triethylene glycol dimethacrylate; UDMA: Urethane dimethacrylate.

Table 2 – *Description of the photo-activation protocols evaluated*

Photo-activation method	**Exposure protocol (light exposure time and irradiance*)**	**Energy density***
High-intensity continuous (HIC)	30 s at 900 mW/cm^2	27 J/cm^2
Low-intensity continuous (LIC)	90 s at 300 mW/cm^2	27 J/cm^2
Soft-start (SS)	15 s at 300 mW/cm^2 → 25 s at 900 mW/cm^2	27 J/cm^2
Pulse-delay (PD)	3 s at 300 mW/cm^2 → Delay (3 min) → 29 s at 900 mW/cm^2	27 J/cm^2

*received at top surface of the specimen.

Table 3 – *Axial shrinkage (mean ± standard deviation in %) of the tested composite materials generated by the photo-activation methods at 15 min after the start of irradiation (n = 6)*

Photo-activation method	Material			
	SDR	**Esthet X flow**	**Esthet X HD**	**Rebilda DC**
High-intensity continuous (HIC)	2.26 ± 0.10 **A,c**	3.40 ± 0.06 **A,a**	1.49 ± 0.05 **A,d**	2.98 ± 0.11 **A,b**
Low-intensity continuous (LIC)	2.22 ± 0.04 **A,c**	3.42 ± 0.10 **A,a**	1.46 ± 0.06 **A,d**	2.96 ± 0.10 **A,b**
Soft-start (SS)	2.29 ± 0.04 **A,c**	3.44 ± 0.11 **A,a**	1.48 ± 0.07 **A,d**	2.86 ± 0.07 **A,b**
Pulse-delay (PD)	2.27 ± 0.07 **A,c**	3.40 ± 0.07 **A,a**	1.39 ± 0.10 **A,d**	2.86 ± 0.12 **A,b**

Mean values followed by same capital letters in columns, and same small letters in rows, are not significantly different at the 0.05 level (Scheffé's post-hoc test).

Table 4 – *Shrinkage force (mean ± standard deviation in N) of the tested composite materials generated by the photo-activation methods at 15 min after the start of irradiation (n = 6)*

Photo-activation method	Material			
	SDR	**Esthet X flow**	**Esthet X HD**	**Rebilda DC**
High-intensity continuous (HIC)	20.0 ± 1.2 **A,c**	40.7 ± 0.9 **A,a**	22.7 ± 0.8 **A,b**	40.4 ± 1.9 **A,a**
Low-intensity continuous (LIC)	19.9 ± 0.9 **A,b**	38.0 ± 1.7 **B,a**	19.6 ± 1.2 **B,b**	36.8 ± 0.8 **B,a**
Soft-start (SS)	19.9 ± 1.1 **A,c**	39.4 ± 1.7 **AB,a**	20.6 ± 0.6 **B,c**	36.0 ± 2.3 **B,b**
Pulse-delay (PD)	17.9 ± 0.7 **B,b**	35.3 ± 1.5 **C,a**	15.5 ± 1.6 **C,c**	35.6 ± 1.5 **B,a**

Mean values followed by same capital letters in columns, and same small letters in rows, are not significantly different at the 0.05 level (Scheffé's post-hoc test).

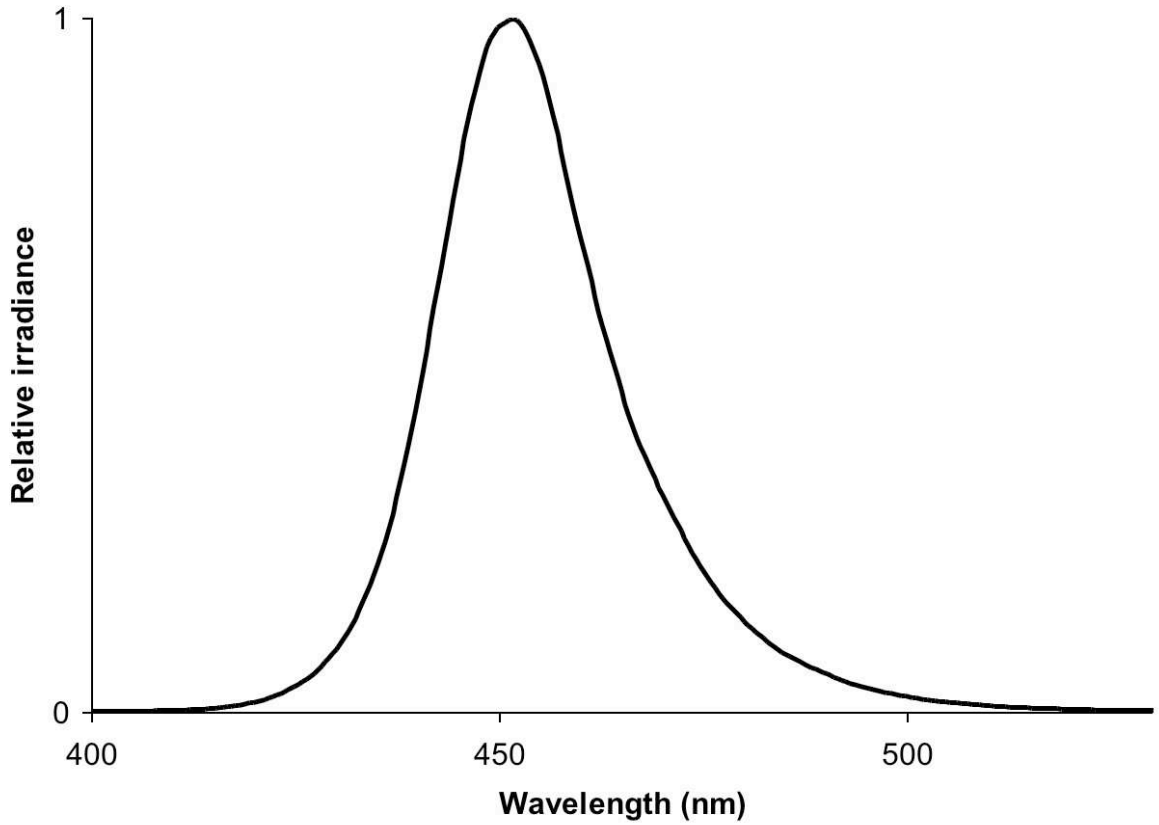

Fig. 1. Light spectrum profile emitted by the LED curing unit (Bluephase; Ivoclar Vivadent) used in the study.

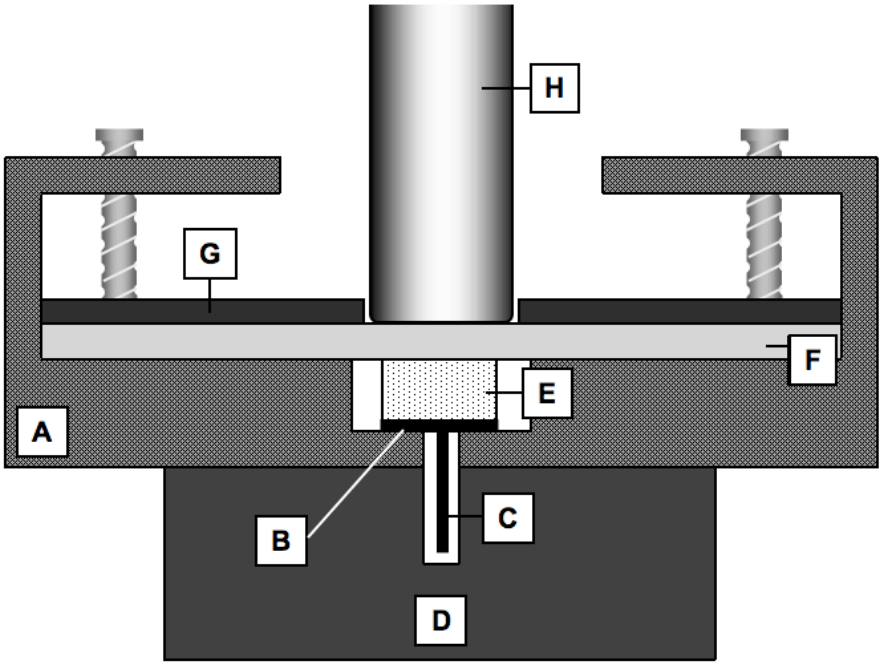

Fig. 2. Diagram of the measuring device for axial shrinkage. A: Metal frame; B: Aluminum platelet; C: Diaphragm; D: Infrared measuring sensor; E: Composite specimen; F: Glass plate; G: Aluminum plate; H: Curing light tip.

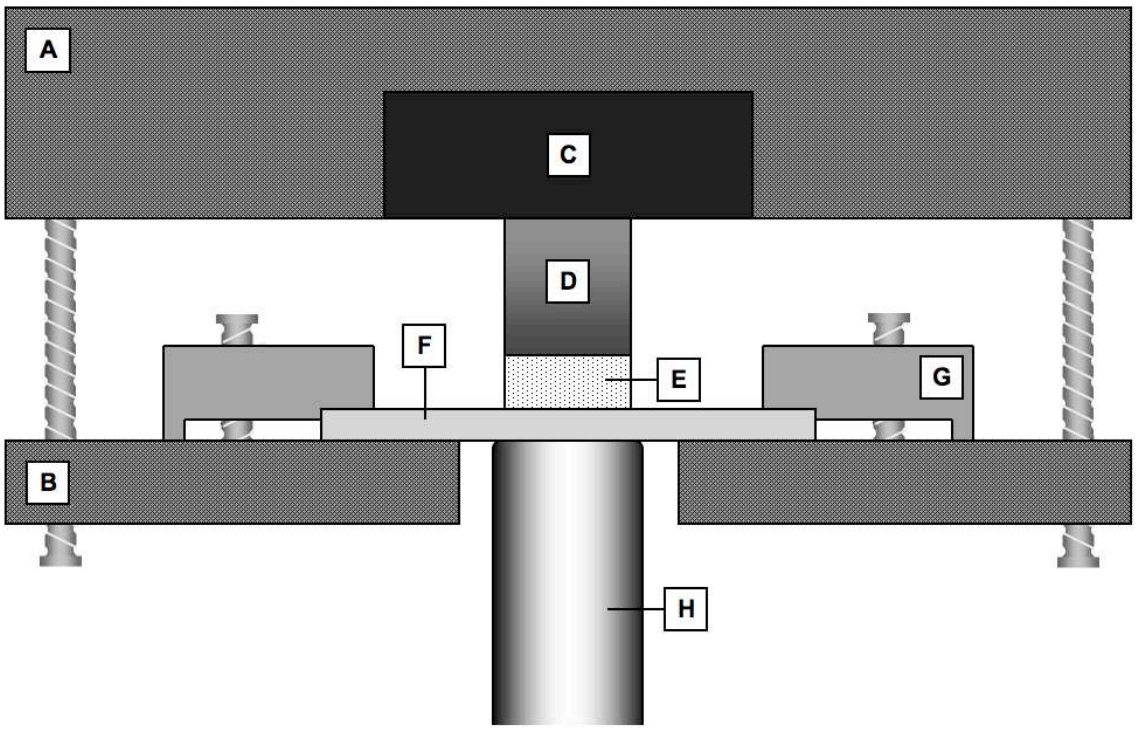

Fig. 3. Diagram of the measuring device for shrinkage force. A: Upper part of measuring device; B: Lower part of measuring device; C: Load cell; D: Metal cylinder; E: Composite specimen; F: Glass plate; G: Holder of glass plate; H: Curing light tip.

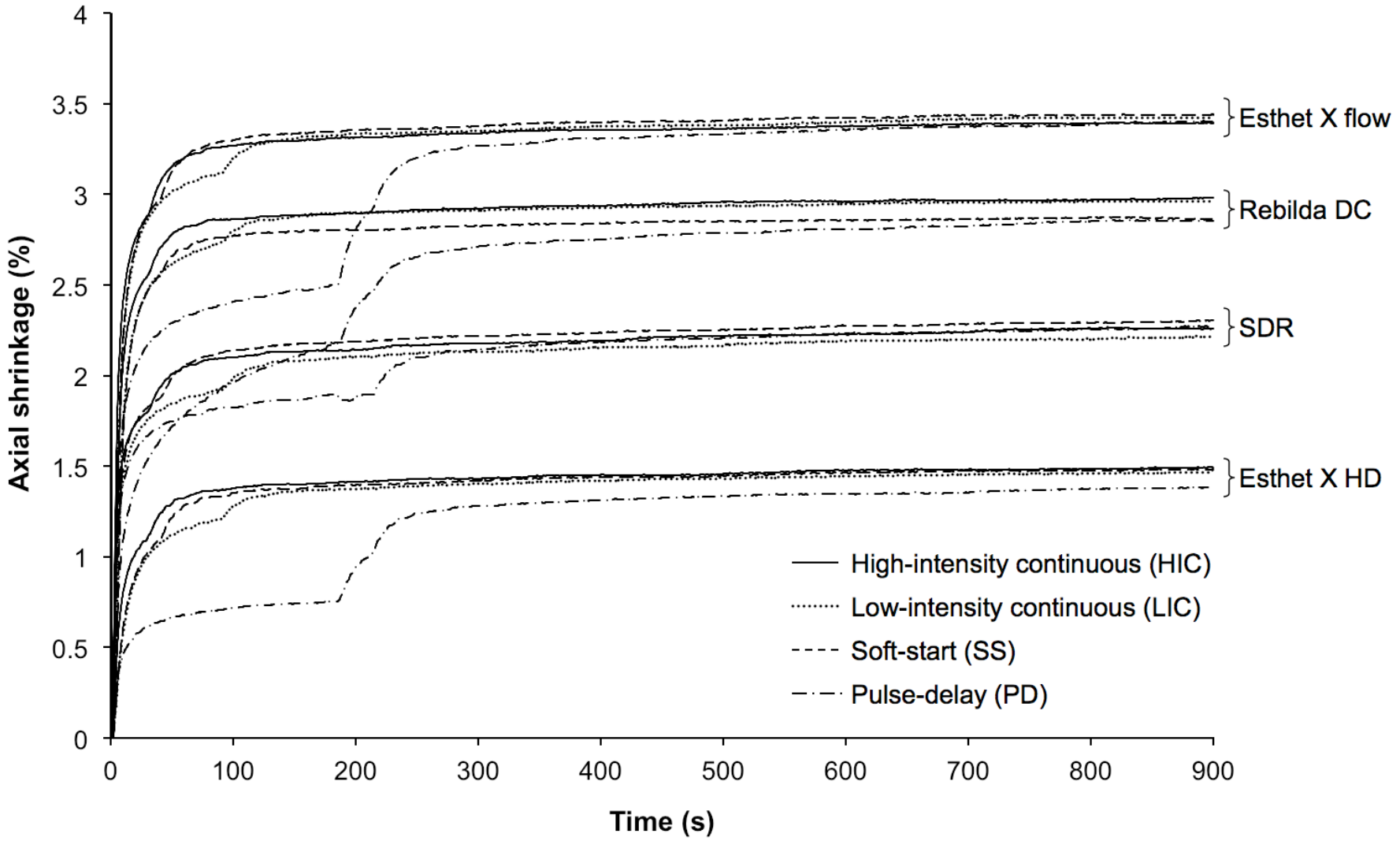

Fig. 4. Mean axial shrinkage curves of the composite materials for each photo-activation method as a function of time (n = 6).

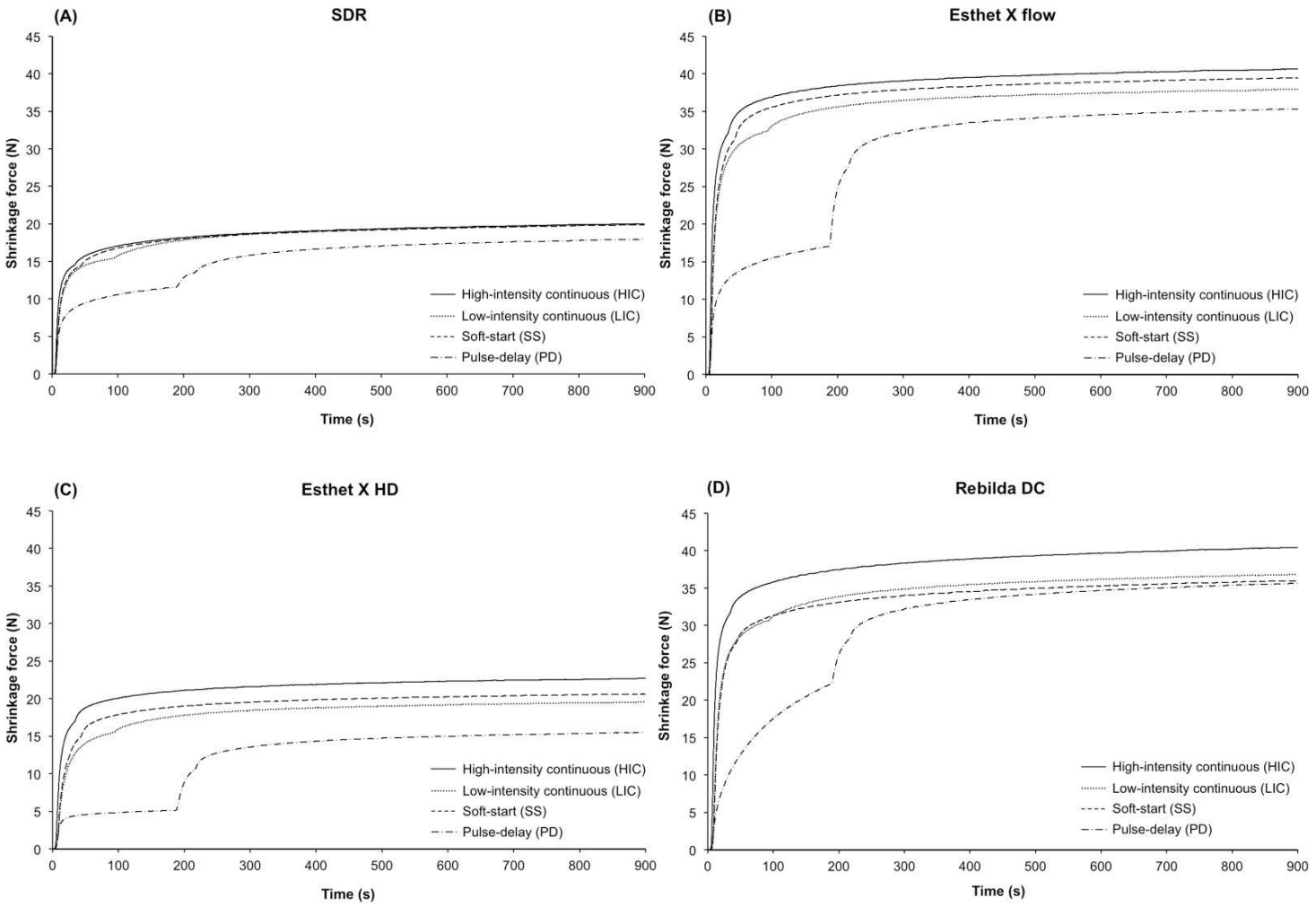

Fig. 5. Mean shrinkage force curves of the composite materials for each photo-activation method as a function of time (n = 6).

(A) SDR; (B) Esthet X flow; (C) Esthet X HD; (D) Rebilda DC.

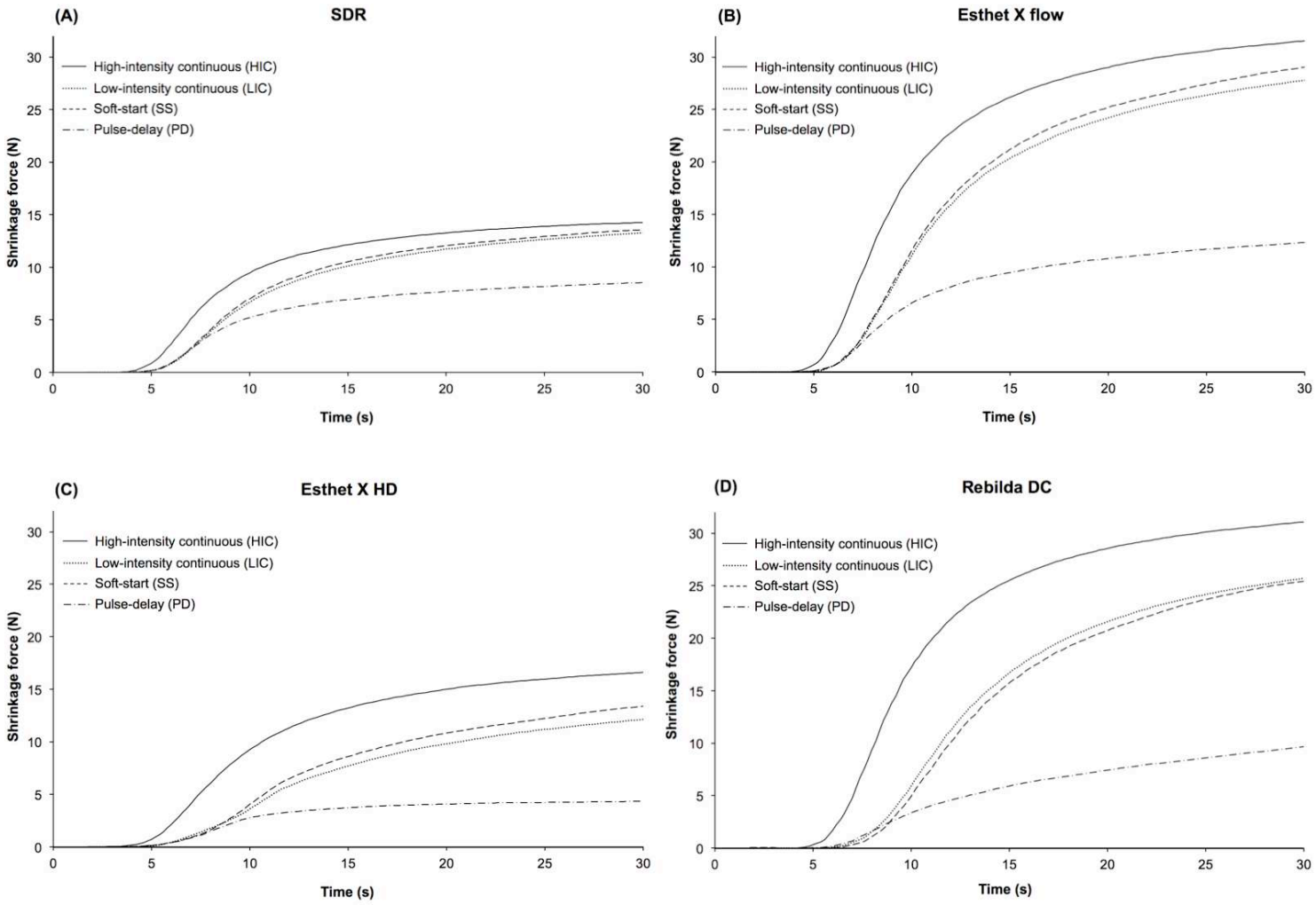

Fig. 6. Mean shrinkage force curves of the composite materials for each photo-activation method within 30 s after the start of irradiation (expanded area of Fig. 5). (A) SDR; (B) Esthet X flow; (C) Esthet X HD; (D) Rebilda DC.

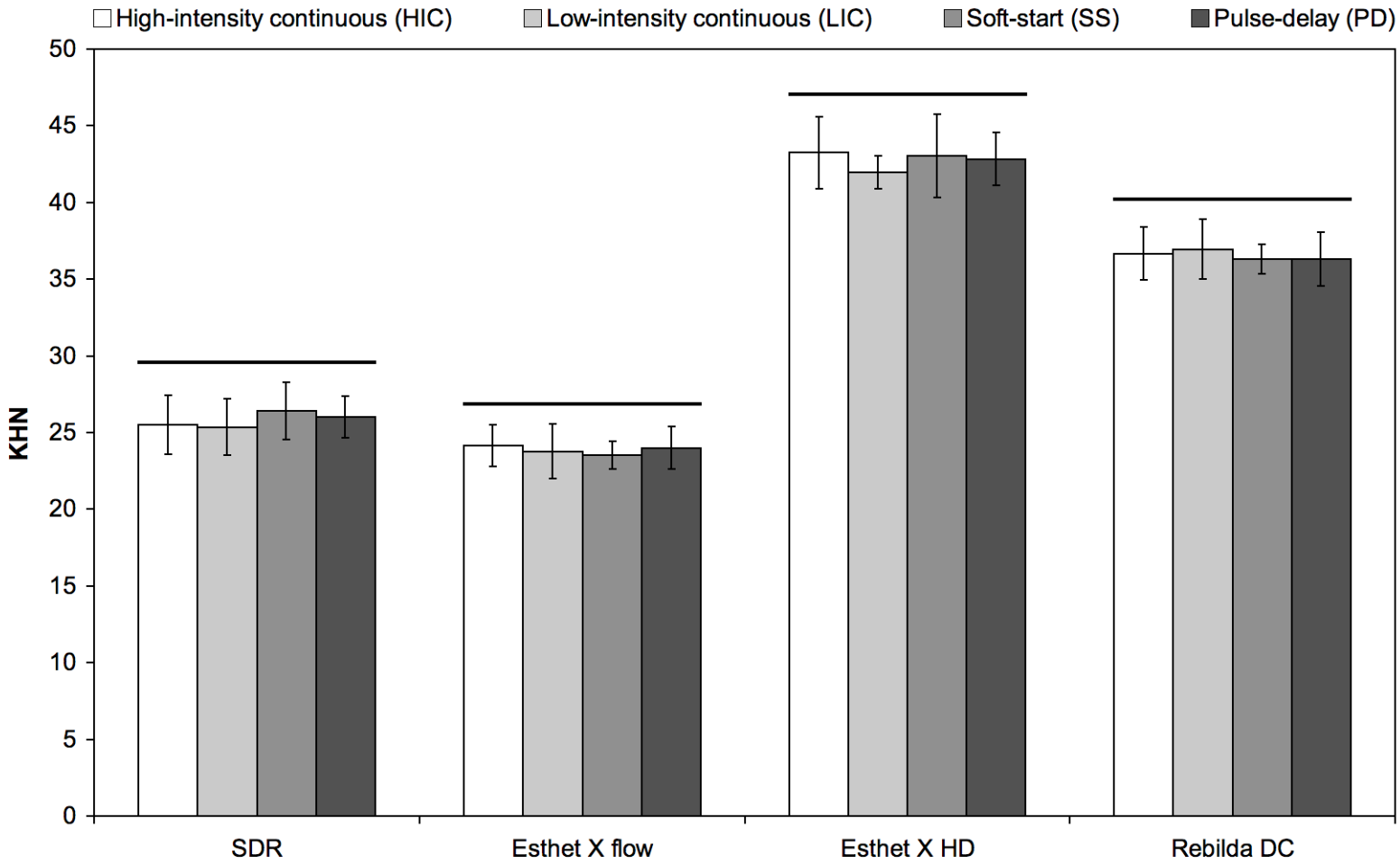

Fig. 7. Mean Knoop hardness values and standard deviations (represented by error bars) of all experimental groups at 15 min after the start of irradiation (n = 6). Within each composite material, groups linked with a horizontal bar are not significantly different at the 0.05 level (Scheffé's post-hoc test).